
This is an electronic reprint of the original article.
This reprint may differ from the original in pagination and typographic detail.

Prabakaran, K.; Jayasakthi, M.; Surender, S.; Pradeep, S.; Sanjay, S.; Ramesh, Raju; Balaji, M.; Gautier, Nicolas; Baskar, K.

Structural, morphological, optical and electrical characterization of InGaN/GaN MQW structures for optoelectronic applications

Published in:
Applied Surface Science

DOI:
[10.1016/j.apsusc.2019.01.156](https://doi.org/10.1016/j.apsusc.2019.01.156)

Published: 15/05/2019

Document Version
Peer-reviewed accepted author manuscript, also known as Final accepted manuscript or Post-print

Published under the following license:
CC BY-NC-ND

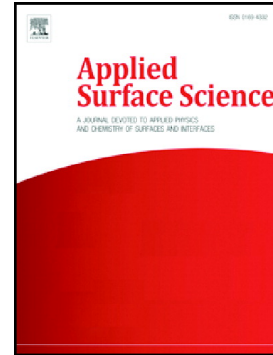
Please cite the original version:
Prabakaran, K., Jayasakthi, M., Surender, S., Pradeep, S., Sanjay, S., Ramesh, R., Balaji, M., Gautier, N., & Baskar, K. (2019). Structural, morphological, optical and electrical characterization of InGaN/GaN MQW structures for optoelectronic applications. *Applied Surface Science*, 476, 993-999.
<https://doi.org/10.1016/j.apsusc.2019.01.156>

This material is protected by copyright and other intellectual property rights, and duplication or sale of all or part of any of the repository collections is not permitted, except that material may be duplicated by you for your research use or educational purposes in electronic or print form. You must obtain permission for any other use. Electronic or print copies may not be offered, whether for sale or otherwise to anyone who is not an authorised user.

Accepted Manuscript

Structural, morphological, optical and electrical characterization of InGaN/GaN MQW structures for optoelectronic applications

K. Prabakaran, M. Jayasakthi, S. Surender, S. Pradeep, S. Sanjay, R. Ramesh, M. Balaji, Nicolas Gautier, K. Baskar



PII: S0169-4332(19)30165-5
DOI: <https://doi.org/10.1016/j.apsusc.2019.01.156>
Reference: APSUSC 41555
To appear in: *Applied Surface Science*
Received date: 8 October 2018
Revised date: 11 January 2019
Accepted date: 18 January 2019

Please cite this article as: K. Prabakaran, M. Jayasakthi, S. Surender, et al., Structural, morphological, optical and electrical characterization of InGaN/GaN MQW structures for optoelectronic applications, *Applied Surface Science*, <https://doi.org/10.1016/j.apsusc.2019.01.156>

This is a PDF file of an unedited manuscript that has been accepted for publication. As a service to our customers we are providing this early version of the manuscript. The manuscript will undergo copyediting, typesetting, and review of the resulting proof before it is published in its final form. Please note that during the production process errors may be discovered which could affect the content, and all legal disclaimers that apply to the journal pertain.

Structural, Morphological, Optical and Electrical Characterization of InGaN/GaN MQW Structures for Optoelectronic Applications

K. Prabakaran^{1*}, M. Jayasakthi¹, S. Surender¹, S. Pradeep¹, S. Sanjay¹, R. Ramesh³, M. Balaji⁴, Nicolas Gautier⁵, K. Baskar^{1,2*}

¹ Crystal Growth Centre, Anna University, Chennai, India

² Manonmaniam Sundaranar University, Tirunelveli, India

³ Department of Electronics and Nanoengineering, Aalto University, Finland

⁴ Department of Energy, University of Madras, Guindy Campus, Chennai, India

⁵ Institut des Matériaux Jean Roused, UMR 6502 CNRS Université de Nantes, France

Abstract

InGaN/GaN Multiple QuantumWell (MQW) structures were grown on *c*-plane sapphire substrate using metal organic chemical vapour deposition technique by varying the MQW periods. The indium composition and thickness were estimated using high-resolution X-ray diffraction. InGaN well, GaN barriers and Indium composition were estimated as 3 nm, 18 nm and 16-18% using epitaxy smooth fit software. Reciprocal space mapping revealed that InGaN/GaN MQW samples were coherently strained. High-resolution transmission electron microscopy images confirmed good interface between the InGaN/GaN MQW structures. Atomic force microscopy and scanning electron microscopy exhibit decrease in the surface roughness with increase in the number of InGaN/GaN MQW periods with respect to the number of defects comprising of threading dislocations and hexagonal V-pits. Self-organized In(Ga)N like nanostructures with spiral growth mechanism was also observed due to the low temperature growth of p-GaN layer. The photoluminescence spectra of the MQWs showed a red-shift when the number of QW periods was increased due to quantum confined stark effect. Hall Effect measurement displayed good semiconducting behavior in the InGaN/GaN MQW structures. The carrier concentration values also emphasized adequate variations when number of periods was increased.

Keywords: InGaN, Multiple Quantum Well, Photoluminescence, V-pits, nanostructures

***Corresponding Author:**

Dr. K. Prabakaran

Crystal Growth Centre

Anna University

Chennai-25, India

E-Mail: karanphy07@gmail.com (K.Prabakaran)

drbaskar2009@gmail.com (K. Baskar)

1. Introduction

Group III-nitride semiconductors have been an excellent candidate for various applications such as optoelectronics and high power devices [1-4]. They are widely preferred for their outstanding tunable direct bandgap characteristics from near infrared ($\sim 0.7\text{eV}$ -InN) to ultraviolet region (GaN-3.4 eV) by varying the Indium (In) compositions [5-8]. Comparing with the other semiconducting materials, InGaN attracts more attention due to its high carrier mobility, superior radiation resistance and high optical absorption ($\sim 10^5\text{cm}^{-1}$) [5, 9-12]. InGaN based optoelectronics devices possess excellent physical and chemical stability that allows them to operate under harsh environments [13, 14]. In general, InGaN/GaN multiple quantumwell (MQW) structures act as active regions for light emitting diode (LED), solarcells and thermoelectric applications. However, extending the emission range (From green to red) and improve the luminescence property of InGaN is still challenge [15]. Furthermore, to minimize the lattice mismatch between InN and GaN to obtain InGaN layer with high crystalline quality is another challenge [6, 16, 17]. In order to surmount this intricacy, the InN layers are generally grown at low temperature (LT) due to the thermal decomposition of InN. The growth of thick InGaN layer with comparatively high indium composition is one of the critical challenges in fabricating InGaN-based optoelectronic devices [18]. To overcome these issues, the In-rich thin

InGaN layer based MQW structure was used as an alternative. The crystalline quality depends on various parameters such as optimization of barrier, well thickness and growth temperature of MQWs [17, 19] along with the In composition of InGaN wells and number of MQW periods. However, the collection of carriers in strained MQWs can be affected considerably by the spontaneous and piezoelectric polarization fields. This phenomenon is known as quantum confinement stark effect (QCSE). It leads to the spatial separation of electron and hole wave functions, which restricts the carrier recombination efficiency [20]. In addition, surface topography of In-rich InGaN based MQW structures aggravates the optical and electrical properties, through high density of structural defects like threading dislocations (TD), V-defects and trench defects during the epitaxial process [21-24]. This also affects the interface of InGaN/GaN MQWs during the growth of p-GaN layers. To avoid such degradation in the quality of InGaN/GaN MQWs, the p-GaN layer is grown at lower temperatures [3, 25]. A better understanding of structural, morphological, optical and electrical properties of InGaN/GaN MQW structure are necessary to achieve sharp interfaces and atomically flat surface, which enhances the efficiency [23]. In the present work, the effects of increasing the number of periods in MQWs and the effect of growing p-GaN layer at low temperature in InGaN/GaN MQW structures have been carried out.

2. Experimental procedure

InGaN/GaN MQW structures were grown on 2-inch *c*-plane sapphire substrate using metal organic chemical vapour deposition (MOCVD, Aixtron200/4RF-S) by varying the period of MQWs. Trimethylgallium (TMGa), Trimethylindium (TMIn) and ammonia (NH₃) were used as precursors for gallium, indium and nitrogen respectively. Triethylgallium (TEGa) was used as the gallium precursor during the growth of barrier layer in the active region of the structures.

Silane and biscyclopentadienyl magnesium (Cp_2Mg) were used as n and p-type dopants respectively. High purity hydrogen (H_2) and nitrogen (N_2) were used as carrier gases. Prior to the growth, the sapphire substrates were thermally cleaned under H_2 ambience at 1050°C for 10 min to remove residues and impurities on the surface. Subsequently, 25 nm thick GaN nucleation layer (NL) was grown at 520°C with a V/III ratio of 3453. GaN NL was then recrystallized at 1000°C for 1 min. The growth temperature was ramped up to 1010°C and a 2 μm thick n-GaN/GaN was grown (carrier concentration - $2.48 \times 10^{18} \text{ cm}^{-3}$) [26] using H_2 . Silane flow rate for Si-GaN layer was maintained at 40 standard cubic centimeters per minute (SCCM) with a V/III ratio of 614. The InGaN/GaN MQW (one, three and five periods) structures comprising of InGaN wells were grown at 720°C with V/III ratio 11625 (TMIn flow-13 $\mu\text{mol}/\text{min}$ & TEGa flow rate – 6.2 $\mu\text{mol}/\text{min}$) and the GaN barriers at 820°C . Finally, Cp_2Mg flow rate for Mg-GaN layer was 300 SCCM grown at 920°C , continue to In-situ annealing at 700°C for 15 min in all samples. Schematic view of the structures has been shown in the figure 1.

The crystalline quality, composition and thickness of the InGaN/GaN MQW structures were determined using High resolution X-ray Diffractometer (HRXRD- PANalytical X'Pert Pro MRD). The morphology of InGaN/GaN MQW and the interfaces were performed using a High resolution transmission electron microscopy (HRTEM) (Hitachi, H-9000-NAR, LaB_6 filament, 300 kV, point to point resolution: 0.18nm). Cross-section TEM samples were prepared by tripod polishing and subsequently polishing it with Ar^+ ion using Gatan precision ion polishing system (PIPS). The surface properties and roughness were analyzed by scanning electron microscopy (SEM, CarlZeiss EVO18), atomic force microscopy (AFM, Park XE-100) respectively. Photoluminescence (PL, Spectra Physics) of the samples were measured at room temperature by 244 nm Ar^+ laser. The electrical properties of the samples were measured using hall measurement system (ECOPIA, HMS 5000).

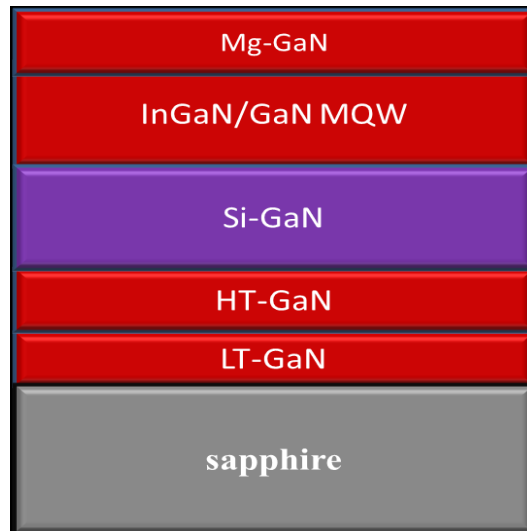


Figure 1. Schematic diagram of the InGaN/GaN MQW structures

3. Results and Discussion

3.1 Structural Analysis

Figure 2 illustrates the ω - 2θ scan of MQW structures were observed using HRXRD. Thicknesses and In compositions of the InGaN MQWs were obtained from the symmetric scans of (0 0 0 2) plane. Using the epitaxy smooth fit software (figure 2 (III)), the InGaN well and GaN barrier thickness were determined as 3 ± 0.5 nm and 18 ± 0.5 nm respectively. The In compositions were estimated around ~ 16-18 %. From the obtained HRXRD results, the high intense peaks manifests that, the grown n-GaN/GaN is oriented along (0 0 0 2) plane. The satellite peaks observed illustrates good periodicity in the MQW layers (figure 2 (II)). It is worth to note that, the absence of satellite peaks in one period InGaN/GaN QW (figure 2(I)), emphasize the non-uniformity in the InGaN/GaN interface which is evident from its surface roughness [27]. The full width at half maximum (FWHM) broadening of three periods InGaN/GaN MQWs improved the crystalline randomization by exposing less interface roughness between InGaN and GaN layers in comparison to one period QW structure [28]. Also, the satellite peak narrowing of five periods InGaN/GaN MQW revealed the interface is atomically flat when compared with the other two

samples (Figure 2(II)). Among the three samples, the InGaN/GaN MQW structures grown at five periods exhibits better crystallinity [29].

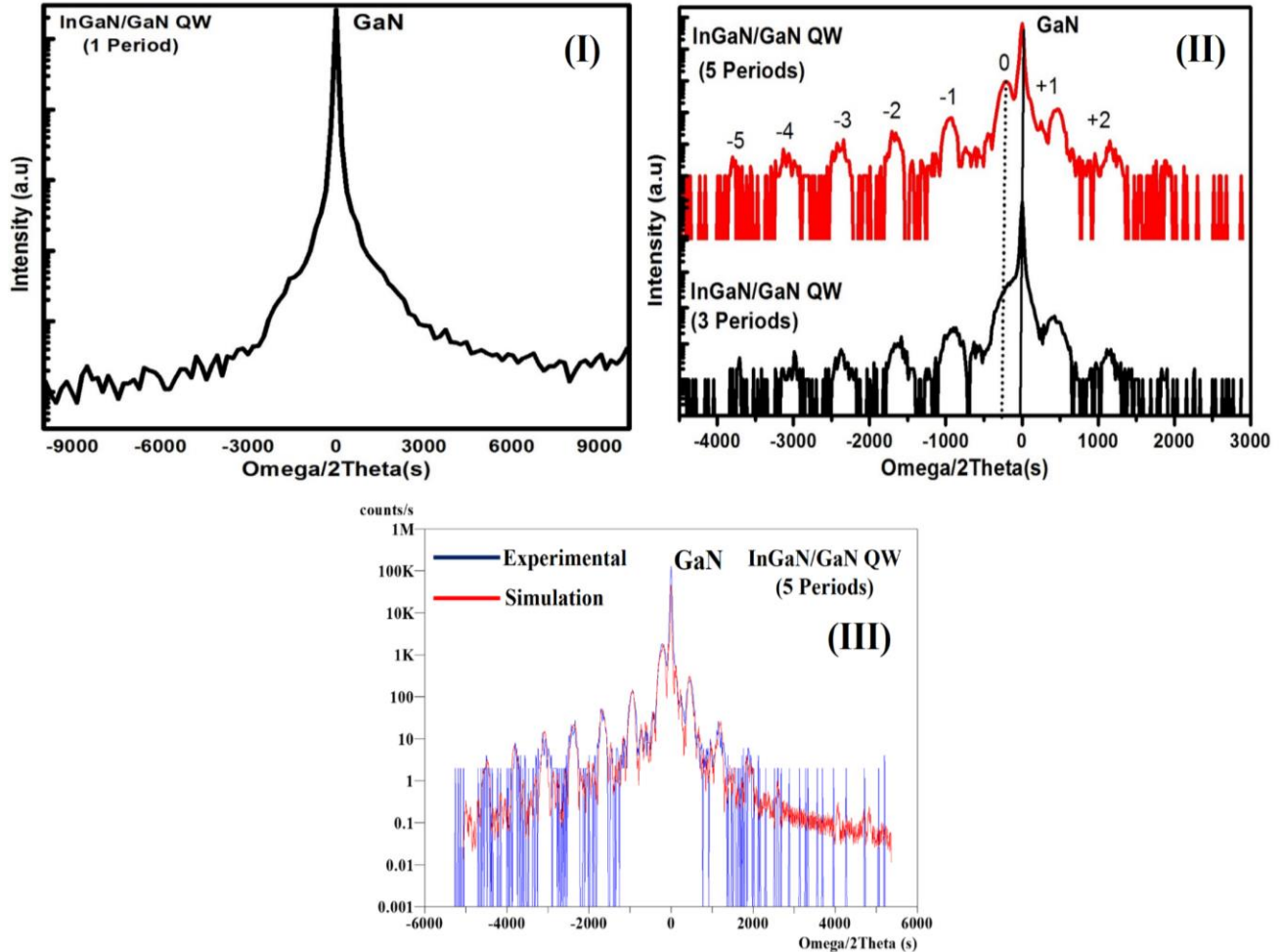


Figure 2. HRXRD (0 0 0 2) plane of (I) InGaN/GaN QW (one period) structure (II) InGaN/GaN MQW (three and five periods) structure (III) InGaN/GaN MQW (five periods) for experimental (Blueline) along with simulation (Redline)

The rocking-curve analysis in respect of GaN was carried out for all the samples. The FWHM of (0 0 0 2) plane rocking curve of GaN are estimated as 400, 370 and 372 arc-sec, whereas for (1 0 -1 5) it is 242, 230 and 246 arc-sec. The TD density was calculated from the below equations [30],

$$D_{edge} = \frac{\beta^2}{4.35|b_{edge}|^2} \quad D_{screw} = \frac{\alpha^2}{4.35|b_{screw}|^2} \quad (1)$$

Where D_{edge} is the edge dislocation density, D_{screw} is the screw dislocation density and α , β refers to FWHM value measured from rocking curve diffraction peaks of (0 0 0 2) and (1 0 -1 5) planes respectively. Here, lattice constant a -axis (0.31878 nm) is the length of the burger vector for the edge dislocation density and c -axis (0.5185 nm) is the length of the burger vector of the screw dislocation density [31]. The calculated TD density of GaN layers of the three samples are shown in table 1. The TD density of GaN was found to be in the range from 6.32×10^8 to $5.99 \times 10^8 \text{ cm}^{-2}$. The TD density in GaN base layer for three periods of InGaN/GaN MQW structure was lesser in comparison to the other two samples. This is attributed to the low tilt and twist disorientations with respect to the screw and edge dislocations originating from n-GaN/GaN layer.

Figure 3 shows the reciprocal space mapping (RSM) corresponding to the asymmetric (1 0 -1 5) plane of InGaN/GaN MQW structures for one, three and five periods respectively. The high intensity GaN peak is observed on the intense contour lines in all the RSM studies and the InGaN/GaN MQW peaks are observed below the GaN peak. Using the epitaxy smooth fit software, the reciprocal lattice point (RLP) of Q_x values was found to be 0.279046 rlu and 0.277604 rlu for the GaN buffer layer and corresponding peaks of three and five periods of InGaN/GaN MQWs respectively which indicates that the GaN layer, InGaN well and GaN barriers which accommodate on an identical in-plane lattice constants. As the critical thickness of the barrier and wells in the InGaN/GaN MQW structures did not exceed, the overlying InGaN MQWs are coherently strained with respect to the GaN base layer [5]. This reveals that the

InGaN/GaN MQWs are pseudomorphic to the GaN layer. The obtained results comply with the Fast Fourier Transformation (FFT) analysis.

Table 1. Summary of GaN dislocation densities in the InGaN/GaN MQW structures

Samples	GaN dislocations in the InGaN/GaN MQW structures		
	Screw dislocations (10^8cm^{-2})	Edge dislocations (10^8cm^{-2})	TD (10^8cm^{-2})
1 period	3.21	3.11	6.32
3 periods	2.75	2.81	5.56
5 periods	2.78	3.21	5.99

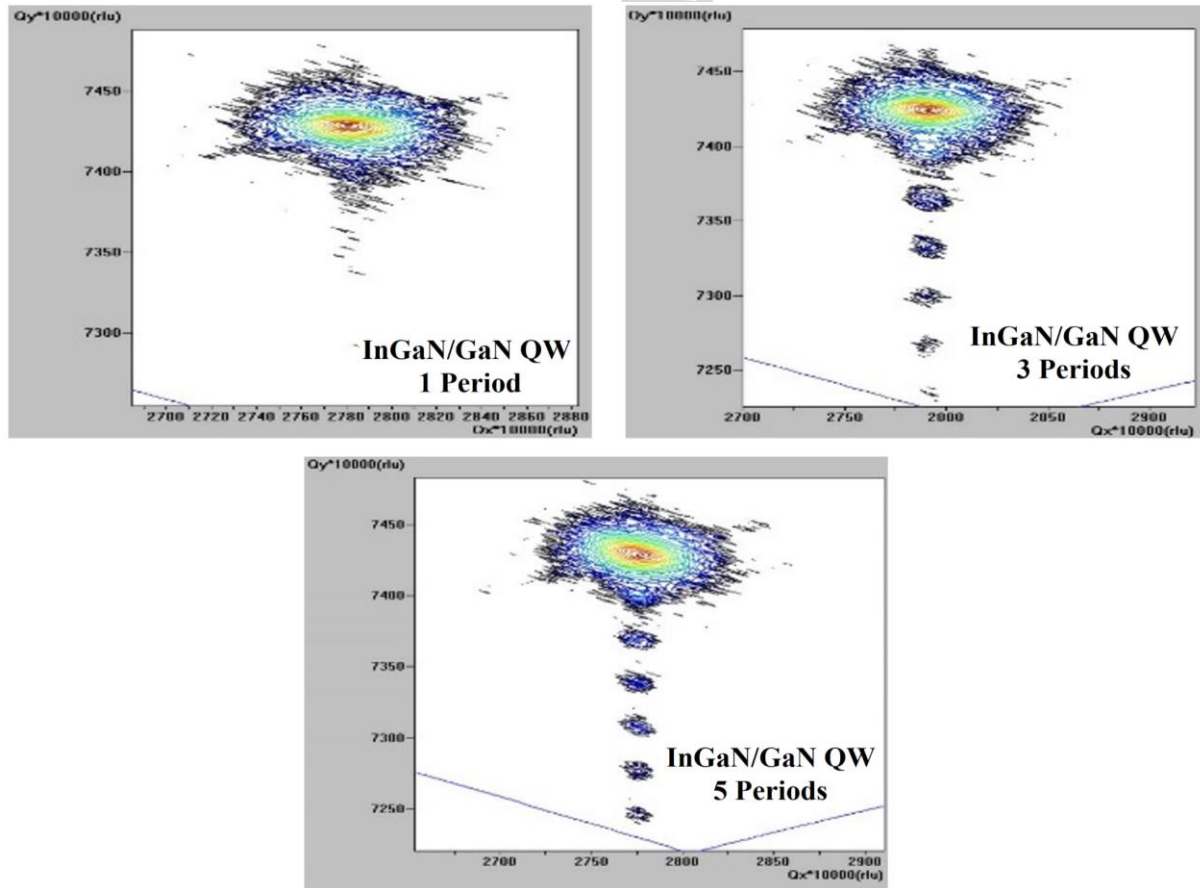


Figure 3. RSM of the InGaN/GaN MQW structures (one, three, and five periods) along (1 0 -1 5) plane

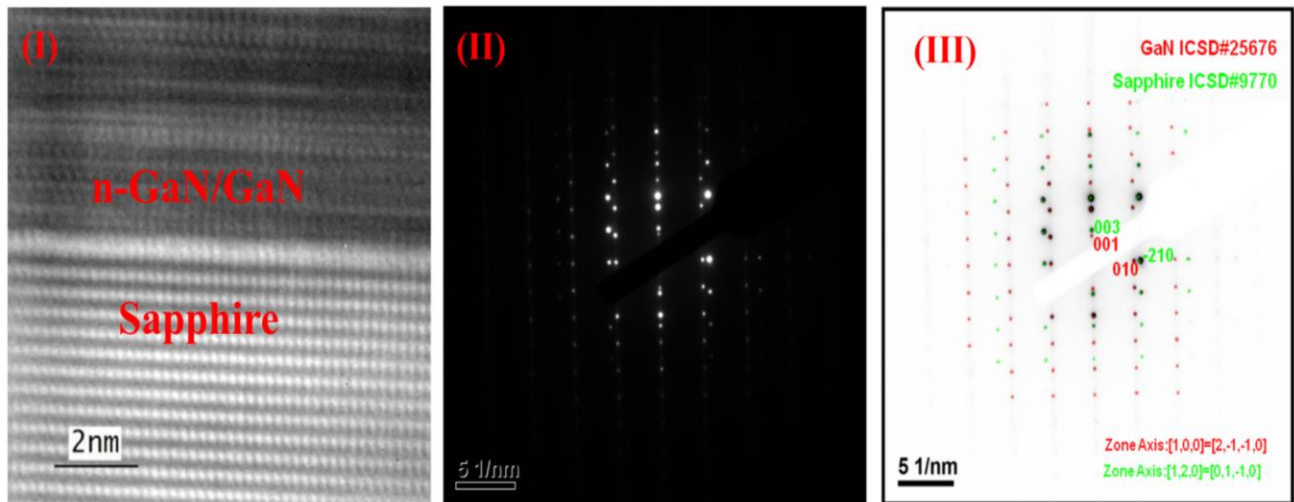


Figure 4. (I) Interface of n-GaN/GaN/Sapphire (II) Corresponding selected area electronic diffractions (SAED) pattern and (III) simulation with JEMS software

Figure 4 represents the cross-sectional HRTEM images of hexagonal GaN (ICSD#25676) layer and sapphire substrate (ICSD#9770) indexed using java electron microscopy software (JEMS) [32]. From Figure, it is clear that, the interface between the layer and substrate is atomically flat. The SAED pattern signifies the epitaxial relationship of hexagonal GaN layer on sapphire substrate. The obtained SAED patterns complement the HRXRD results. The GaN/InGaN/GaN interface has exhibited surface morphology that is predominantly free from pits and stacking faults. The cross-sectional bright field TEM images figure 5 (I, II) show high resolution image of InGaN/GaN MQW (three periods) which further displays the interfaces between the InGaN well (dark) and GaN (bright) barrier layer in InGaN/GaN MQW structures. The thickness of InGaN well and GaN barrier was estimated to be 3 nm and 20 nm respectively. Figure 5 (III) shows indexing of the FFT with both InGaN and GaN layers. The image shows continuous lattice fringes across the GaN/InGaN/GaN interfaces, with no evidences of a misfit layer formation. FFT analysis confirms that the lattice plane alignments are similar in respect of both InGaN and GaN layers [33]. The zone axis corresponding to GaN and InGaN layers were found similar to that of the growth direction.

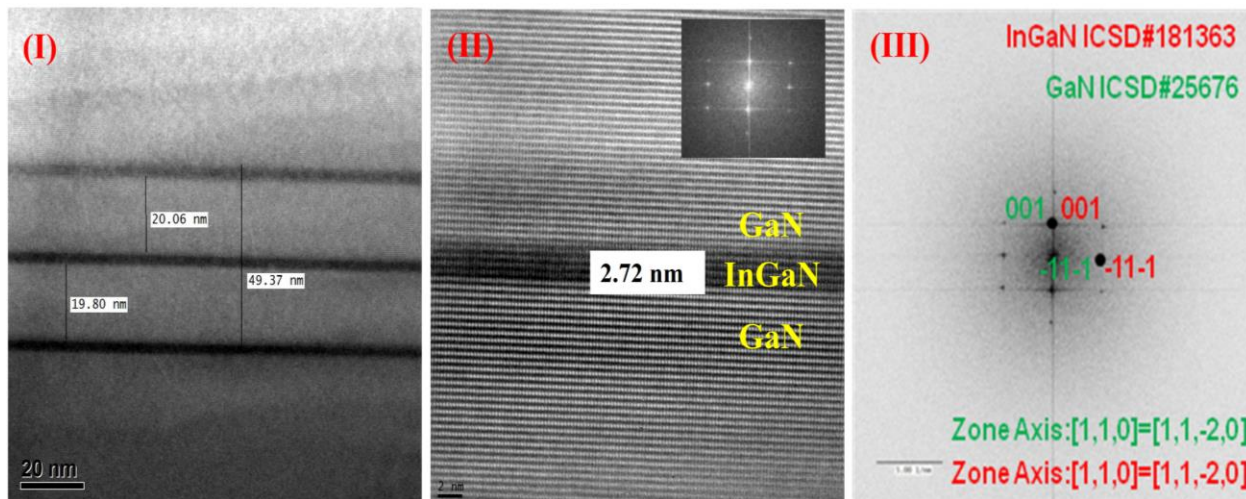


Figure 5. (I) GaN/InGaN/GaN interfaces representing InGaN/GaN MQW structures (three periods) (II) High resolution TEM of GaN/InGaN/GaN interfaces in three periods of InGaN/GaN MQW structures and corresponding FFT (Inset View) (III) Simulation of JEMS software in InGaN and GaN

3.2 Morphological Analysis

Figure 6 shows the sequence of AFM images comprising of InGaN/GaN MQW (one, three and five periods) structures respectively. The smooth and roughened surfaces of the p-GaN samples were clearly observed. These surface roughnesses of p-GaN can be attributed to TDs intersecting the active layer and the formation of Mg-H complexes in p-GaN layer [34]. The roughness of the p-GaN surface decreases the reflection at the p-GaN/air interface which in turn increases the path light through the active region thereby increasing the light absorption of these structures. Rough p-GaN surface usually grows at low temperature, leading to a high growth rate that result in the formation of V-pits [5]. As represented by the $2 \mu\text{m}^2$ scans of AFM images, the p-GaN surface was characterized by spiral growth along with self-organized In(Ga)N like nanostructures and shallow type V-pits for one and three periods of InGaN/GaN MQW structures. The five periods of InGaN/GaN MQW structures showed step flow growth besides suppressing the nanostructures on the top of p-GaN layer. The root-mean-squared (RMS) roughness as 0.52 nm, 0.26 nm and 0.145 nm were observed for one, three and five periods

respectively. In contrary, the $5\ \mu\text{m}^2$ AFM image for five periods showed significantly rough p-GaN surface with deep V-pits with considerably large RMS roughness of 29 nm. Figure 7 (I) shows the line profile with the pit around 1-2 μm . The observed V-pits were initiated on the TD intersection along the InGaN/GaN QW above the GaN layer (TD density $\sim 10^8\ \text{cm}^{-2}$). The depth of the pit was estimated to be 90-100 nm.

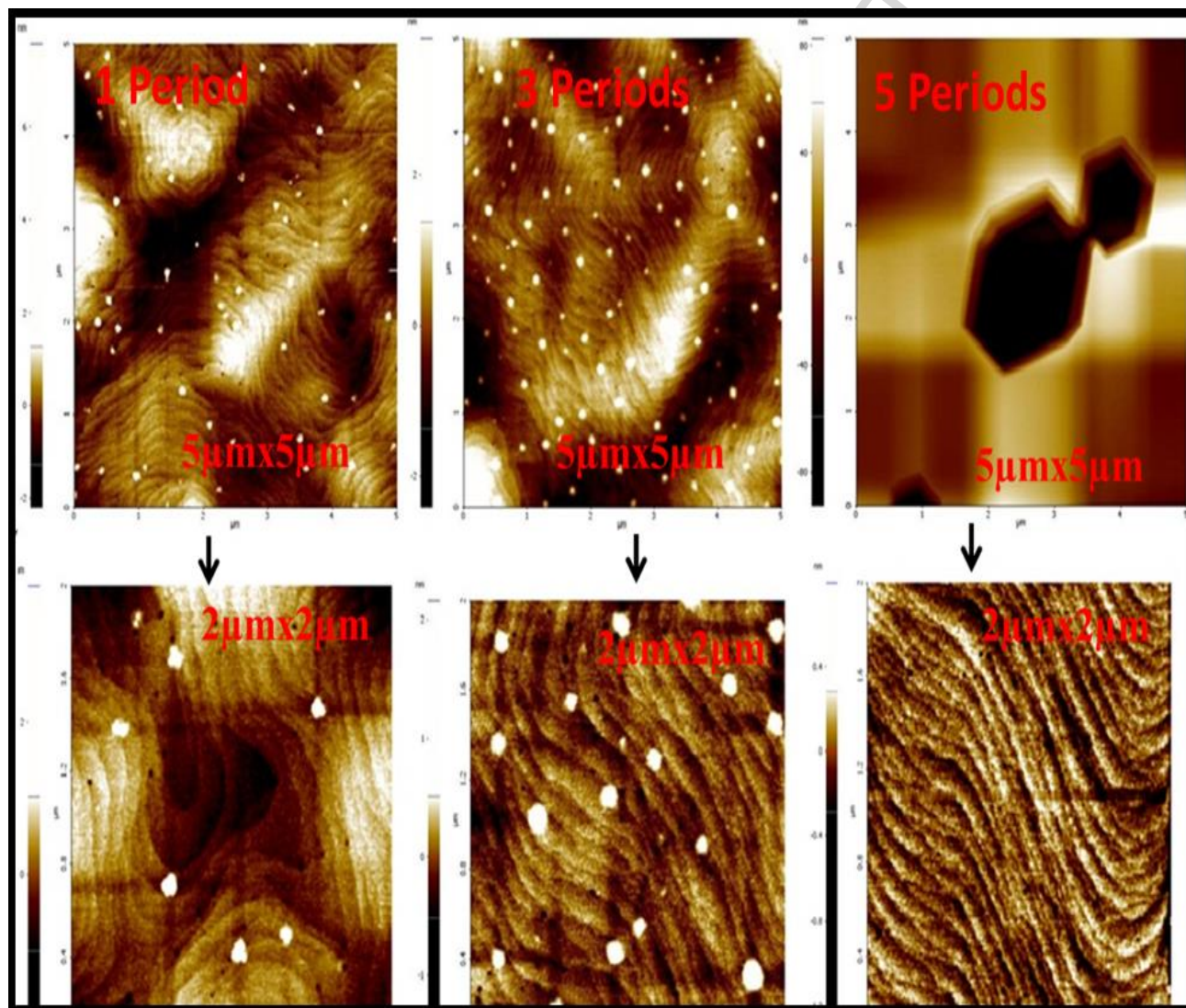


Figure 6. AFM ($5\ \mu\text{m}^2$ and $2\ \mu\text{m}^2$) images depicting InGaN/GaN MQW (one, three and five period) structures

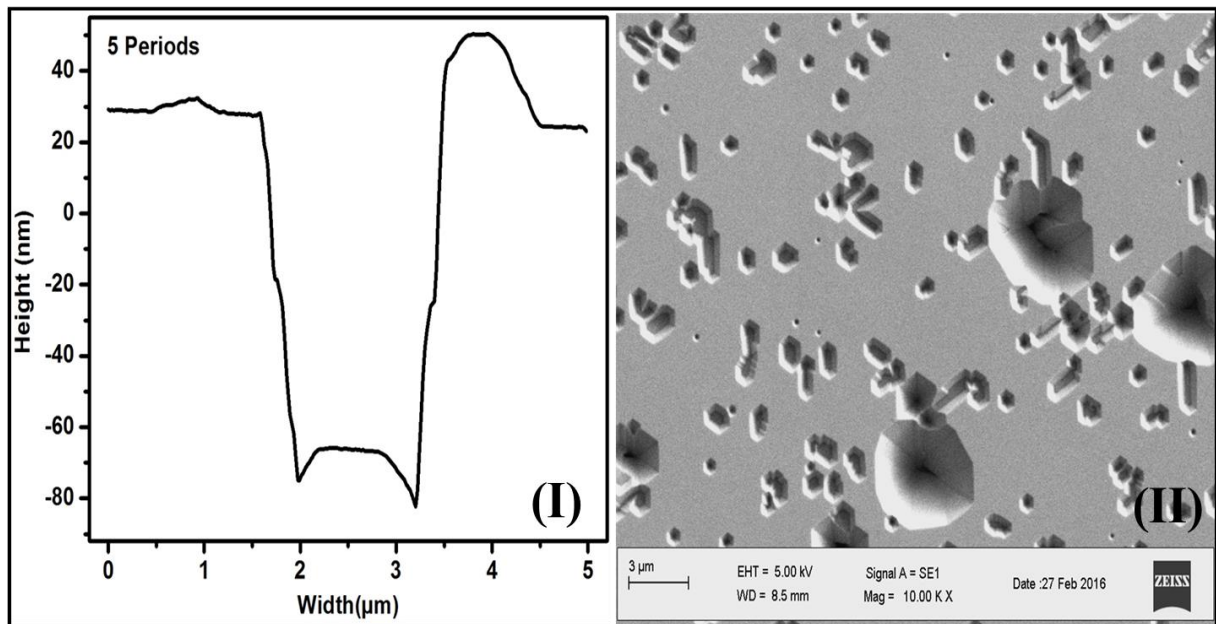


Figure 7. (I) Line profile obtained from AFM images for five periods
(II) SEM images corresponding to (I)

From the figure 7 (ii), the smaller and larger V-pits were observed from the SEM images for InGaN/GaN MQWs (Five periods) samples. The V-pit density was calculated and found to be in the order of $0.16 \times 10^8 \text{ cm}^{-2}$ (figure 7 (II)). The smaller V-pits were due to the edge TDs and larger V-pits compounds to screw or mixed TDs [35]. This emphasizes that the densities of the V-pits corroborates to the results calculated (TD density) from HRXRD.

3.3 Optical Analysis

Room temperature PL spectra for the InGaN/GaN MQW structures for different periods were shown in figure 8. Near band edge emission (NBE) occurs at 363 nm for the n-GaN/GaN layer in all samples. The emissions of InGaN/GaN MQW structure were observed at 479 nm, 480 nm and 505 nm for single, three and five periods respectively. These peak emissions were found to be red shifted in the InGaN/GaN MQW structures which could be attributed to the QCSE resulting of the modification in polarization effect [36, 37]. The PL peaks at 479 nm and 480 nm wavelength displays poor emission intensity caused by self-organized In(Ga)N like

nanostructures. It is worth to note that, the emission at around 383 nm (3.2 eV) is usually occurs for highly Mg-doped GaN that is attributed to the transition between the Mg acceptor (Mg_{Ga}) and deep compensating donor of $Mg_{Ga}-V_N$ complex. However, this does not clearly emerge from the PL spectra due to the lower Mg incorporation and partially reduced nitrogen concentration in single and three periods of the InGaN/GaN MQW structures respectively [38].

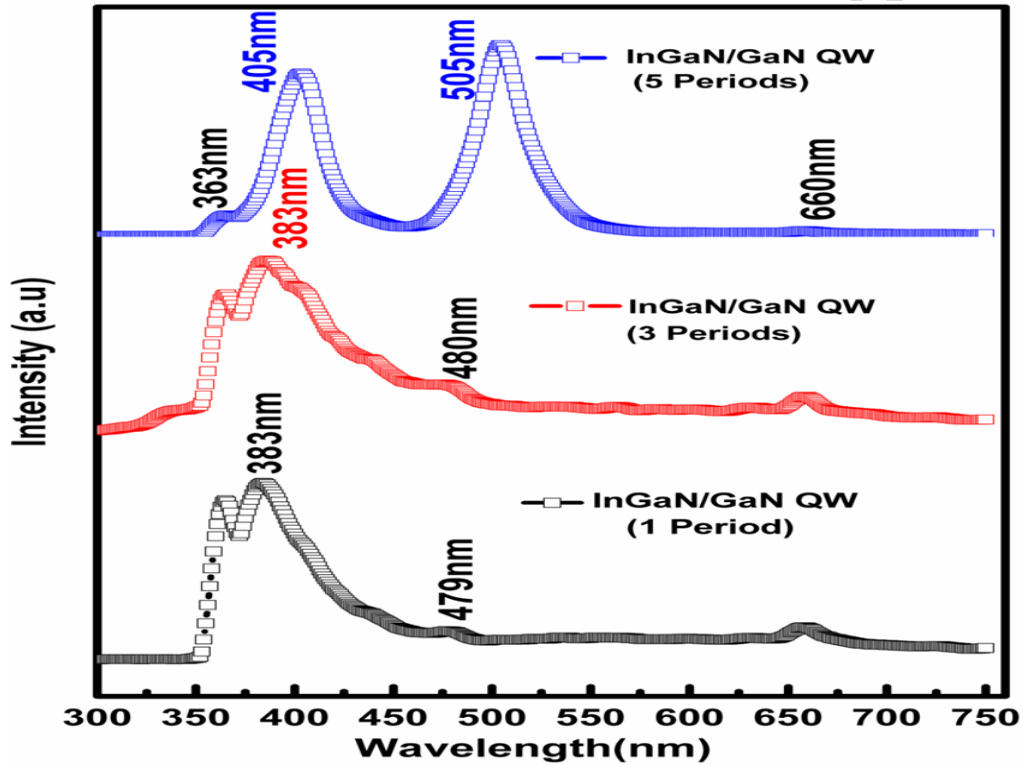


Figure 8. Photoluminescence spectra of InGaN/GaN MQW structures for different periods

The high intense green luminescence peak observed at 505 nm may be due to the dislocations and pits on the surface of five period's sample. The Mg and related transitions shift to 405 nm (3 eV) in the Mg doped GaN layers for five period of InGaN/GaN MQW structures, implying enhancement in the Mg incorporation. This could be attributed to the decrease in the self-compensation effect of native donors and Mg atoms [39]. One could understand from the

above result that the intensity of the red (660 nm) luminescence is an effect of the strong exciton localization on In-rich small regions in the QW interfaces of InGaN/GaN MQW structures [40].

3.4 Electrical Analysis

Table 2. Electrical properties of the InGaN/GaN MQW structures for different Periods

Samples	Mobility cm ² /volt sec	Carrier concentration cm ⁻³	Resistivity ohm-cm
	RT	RT	RT
1 Period	290	2.26x10 ¹⁸	0.0095
3 Periods	275	2.43X10 ¹⁸	0.0093
5 Periods	270	2.30X10 ¹⁸	0.0099

The mobility, carrier concentration and resistivity of the low temperature p-GaN with a Cp₂Mg flow rate of 300 SCCM in respect of the number of periods of the InGaN/GaN MQW structures are shown in table 2. The carrier concentration increases from 2.26x10¹⁸ to 2.43X10¹⁸ cm⁻³ for one and three periods of InGaN/GaN MQW structures. However, the carrier concentration decreases for the five periods of the InGaN/GaN MQW structures. The carrier concentration ~ 10¹⁸ cm⁻³ range point towards the Mg doped GaN related band around 3-3.2 eV [41]. The mobility of the samples were found to decrease gradually as 290, 275, 272 cm²/volt sec for one, three and five periods of InGaN/GaN MQW structures respectively. In the present case, the mobility of low temperature Mg doped GaN was higher when compared to the high temperature p-GaN. Nevertheless, this condition is only applicable for the Cp₂Mg flow rate is less than 500 SCCM [42]. As summarized in table 2, high resistive nature of five periods in

InGaN/GaN MQW structures was observed in comparison to the other two samples (one and three periods). Additionally, it revealed the semiconducting behavior for the all samples.

4. Conclusion

In the present study, InGaN/GaN MQW structures were grown by MOCVD on sapphire substrates. The thickness, composition of InGaN well and GaN barriers have been estimated using HRXRD. The InGaN and GaN thicknesses are correlated by cross sectional HR-TEM. FFT analysis demonstrated the GaN/InGaN/GaN lattice plane alignments along the growth direction. From the asymmetric (1 0 -1 5) plane RSMs, it was found that the InGaN/GaN MQWs were grown as a coherently strained on the underlying n-GaN/GaN layer. The results indicate that five periods of InGaN/GaN MQWs has better surface interface and crystalline quality. PL study revealed the high intensity green emission in InGaN/GaN MQW (five periods) structures. From AFM results, it was observed that the width and depth of the V pits increases with increasing of InGaN/GaN MQWs periods. Also step flow growth initiations in the top of p-GaN layer on InGaN/GaN MQWs (five periods) were revealed. This can be attributed to the suppression of self-organized In(Ga)N like nanostructures and spiral growth mechanism. Hall measurement results revealed the semiconductor behavior as an effect of increasing the number of the periods in InGaN/GaN MQW structures. This work helps us to understand the growth of InGaN/GaN MQWs structures and its structural, morphological, optical and electrical properties. It can be suitable for the fabrication of high efficiency optoelectronic devices.

Acknowledgement

The authors gratefully to acknowledge Department of Science and Technology (DST/TM/SERI/2K12/71(G)), Government of India for funding the research project.

References

- [1] Damilano, B., and Gil, B, Yellow–red emission from (Ga, In) N heterostructures, *J. Phys. D: Appl. Phys*, 48(40), (2015) 403001
- [2] Matioli, E., Neufeld, C., Iza, M., Cruz, S. C., Al-Heji, A. A., Chen, Xu., Farrell, R.M., Keller, S., DenBaars, S., Mishra, U, Nakamura, S, James Speck, and Claude Weisbuch, High internal and external quantum efficiency InGaN/GaN solarcells, *Appl. Phys. Lett*, 98(2), (2011) 021102
- [3] Farrell, R. M., Al-Heji, A. A., Neufeld, C. J., Chen, X., Iza, M., Cruz, S. C., Keller, S, Nakamura, S, DenBaars, S, P, Mishra, U. K and Speck, J. S, Effect of intentional p-GaN surface roughening on the performance of InGaN/GaN solarcells, *Appl. Phys. Lett*, 103(24), (2013) 241104
- [4] Yang, C. C., Sheu, J. K., Liang, X. W., Huang, M. S., Lee, M. L., Chang, K. H., Tu, S. J, Feng-Wen Huang and Lai, W. C. Enhancement of the conversion efficiency of GaN-based photovoltaic devices with AlGaIn/InGaIn absorption layers. *Appl. Phys. Lett*, 97(2), (2010) 021113
- [5] Farrell, R. M., Neufeld, C. J., Cruz, S. C., Lang, J. R., Iza, M., Keller, S., Nakamura, S, DenBaars, S. P, Mishra U. K and Speck, J. S, High quantum efficiency InGaIn/GaN multiple quantum well solarcells with spectral response extending out to 520 nm, *Appl. Phys. Lett*, 98(20), (2011) 201107
- [6] Seo, T. H., Shim, J. P., Chae, S. J., Shin, G., Kim, B. K., Lee, D. S., Young Hee Lee and Suh, E. K, Improved photovoltaic effects in InGaIn-based multiple quantum well solarcell with graphene on indium tin oxide nanodot nodes for transparent and current spreading electrode, *Appl. Phys. Lett*, 102(3), (2013) 031116
- [7] Jeng, M. J., and Lee, Y. L, Increasing solar efficiency of InGaIn/GaN multiple quantum well solar cells with a reflective aluminum layer or a flip-chip structure, *J. Electrochem.Soc* 159(5), (2012) H525-H528
- [8] Seo, D. J., Shim, J. P., Choi, S. B., Seo, T. H., Suh, E. K., and Lee, D. S, Efficiency improvement in InGaIn-based solarcells by indium tin oxide nanodots covered with ITO films, *Opt. express*, 20(106), (2012) A991-A996
- [9] Dahal, R., Li, J., Aryal, K., Lin, J. Y., and Jiang, H. X, InGaIn/GaN multiple quantum well concentrator solarcells, *Appl. Phys. Lett*, 97(7), (2010), 073115

- [10] Pantzas, K., El Gmili, Y., Dickerson, J., Gautier, S., Largeau, L., Mauguin, O., Patriarche, G, Suresh, S, Moudakir, T, Bishop, C, and Ahaitouf, A. Semibulk InGaN: A novel approach for thick, single phase, epitaxial InGaN layers grown by MOVPE. *J. Cryst. Growth*, 370, (2013) 57-62
- [11] Cai, X. M., Wang, Y., Li, Z. D., Lv, X. Q., Zhang, J. Y., Ying, L. Y., and Zhang, B. P, Improved photovoltaic performance of InGaN/GaN solar cells with optimized transparent current spreading layers, *Appl. Phys. A*, 111(2), (2013) 483-486
- [12] Sang, L., Liao, M., Ikeda, N., Koide, Y., and Sumiya, M, Enhanced performance of InGaN solarcell by using a super-thin AlN interlayer, *Appl. Phys. Lett*, 99(16), (2011) 161109
- [13] Valdueza-Felip, S., Mukhtarova, A., Pan, Q., Altamura, G., Grenet, L., Durand, C., Catherine Bougerol, David Peyrade, Fernando González-Posada, Joel Eymery and Monroy, E, Photovoltaic response of InGaN/GaN multiple-quantumwell solar cells, *Jpn. J. Appl. Phys*, 52(8S), (2013) 08JH05
- [14] Sang, L., Liao, M., Koide, Y., and Sumiya, M, InGaN-based thin film solar cells: Epitaxy, structural design, and photovoltaic properties, *J. Appl. Phys*, 117(10), (2015) 105706
- [15] Woo, H., Kim, J., Cho, S., Jo, Y., Roh, C.H., Lee, J.H., Seo, Y.G., Kim, H., Im, H. and Hahn, C.K., Epitaxial growth of low temperature GaN using metal migration enhanced epitaxy for high-quality InGaN/GaN heterojunctions, *Superlattices Microstruct*, 120, (2018), 781-787
- [16] Mahala, P., Singh, S., Pal, S., Singh, K., Chauhan, A., Kumar, P., and Dhanavantri, C, Fabrication and characterization of GaN/InGaN MQW solar cells, *Appl. Phys. A*, 122(7), (2016) 1-6
- [17] Xiao-Bin, Z., Xiao-Liang, W., Hong-Ling, X., Cui-Bai, Y., Qi-Feng, H., Hai-Bo, Y., Chen Hon and Zhan-Guo, W, InGaN/GaN multiple quantum well solar cells with an enhanced open-circuit voltage, *Chin. Phys B*, 20(2), (2011) 028402
- [18] Tsai, Y. L., Wang, S. W., Huang, J. K., Hsu, L. H., Chiu, C. H., Lee, P. T., Peichen Yu, Chien-Chung Lin and Kuo, H. C, Enhanced power conversion efficiency in InGaN-based solar cells via graded composition multiple quantum wells, *Opt. express*, 23(24), (2015) A1434-A1441

- [19] Bai, J., Yang, C. C., Athanasiou, M., and Wang, T, Efficiency enhancement of InGaN/GaN solarcells with nanostructures, *Appl. Phys. Lett*, 104(5), (2014) 051129
- [20] Su, V.C., Chen, P.H., Lin, R.M., Lee, M.L., You, Y.H., Ho, C.I., Chen, Y.C., Chen, W.F. and Kuan, C.H., Suppressed quantum-confined Stark effect in InGaN-based LEDs with nano-sized patterned sapphire substrates, *Opt. express*, 21(24), (2013) pp.30065-30073
- [21] Sheen, M. H., Kim, S. D., Lee, J. H., Shim, J. I., and Kim, Y. W, V-pits as Barriers to Diffusion of Carriers in InGaN/GaN Quantum Wells, *J. Electron. Mater.*, 44(11), (2015) 4134-4138
- [22] Massabuau, F. P., Trinh-Xuan, L., Lodié, D., Thrush, E. J., Zhu, D., Oehler, F., Zhu, M. J, Kappers, C. J, Humphreys and Oliver, R. A, Correlations between the morphology and emission properties of trench defects in InGaN/GaN quantum wells, *J. Appl. Phys*, 113(7), (2013) 073505
- [23] Kumar, M. S., Lee, Y. S., Park, J. Y., Chung, S. J., Hong, C. H., and Suh, E. K, Surface morphological studies of green InGaN/GaN multi-quantum wells grown by using MOCVD, *Mater. Chem. Phys*, 113(1), (2009) 192-195
- [24] Tsai, S.C., Li, M.J., Fang, H.C., Tu, C.H. and Liu, C.P., Efficiency Enhancement of blue light emitting diodes by eliminating V-defects from InGaN/GaN multiple quantum well structures through GaN capping layer control, *Appl. Surf. Sci*, 439, (2018) 1127-1132
- [25] Arif, M., Salvestrini, J. P., Streque, J., Jordan, M. B., El Gmili, Y., Sundaram, S., Xin Li, Gilles Patriarche, Paul L. Voss and Ougazzaden, A, Role of V-pits in the performance improvement of InGaN solar cells, *Appl. Phys. Lett*, 109(13) (2016) 133507
- [26] Prabakaran, K., Jayasakthi, M., Surender, S., Pradeep, S., Sanjay, S., Ramesh, R., Balaji, M. and Baskar, K., Investigations on morphology, growth mode and indium incorporation in MOCVD grown InGaN/n-GaN heterostructures, *Optik*, 175, (2018) 154-162
- [27] Sun, X., Li, D., Song, H., Chen, Y., Jiang, H., Miao, G., and Li, Z, Short- wavelength light beam in situ monitoring growth of InGaN/GaN green LEDs by MOCVD, *Nanoscale res. lett*, 7(1), (2012) 1-6
- [28] Nee, T. E., Shen, H. T., Wang, J. C., and Lin, R. M, Characterization of Berthelot-type behaviors of InGaN/GaN semiconductor heterosystems, *J. Cryst. Growth*, 287(2), (2006) 468-471

- [29] Ren, Z., Chao, L., Chen, X., Zhao, B., Wang, X., Tong, J., Jun Zhang, Xiangjing Zhuo, Danwei Li, and Hanxiang Yiand Li, S, Enhanced performance of InGaN/GaN based solarcells with an $\text{In}_{0.05}\text{Ga}_{0.95}\text{N}$ ultra-thin inserting layer between GaN barrier and $\text{In}_{0.2}\text{Ga}_{0.8}\text{N}$ well, *Opt. express*, 21(6), (2013) 7118-7124
- [30] Lazarev, S, Bauer, S, Forghani, K, Barchuk, M, Scholz, F and Baumbach, T, High resolution synchrotron X-ray studies of phase separation phenomena and the scaling law for the threading dislocation densities reduction in high quality AlGaN heterostructures, *J. Cryst. Growth*, 370, (2013) 51-56
- [31] Choi, S., Heller, E., Dorsey, D., Vetury, R., and Graham, S, Analysis of the residual stress distribution in AlGaN/GaN high electron mobility transistors, *J. Appl. Phys*, 113(9) (2013) 093510
- [32] Stadelmann P, JEMS Java Electron Microscopy Software-<http://cime.epfl.ch/> (2004)
- [33] Ougazzaden, A., Rogers, D. J., Teherani, F. H., Orsal, G., Moudakir, T., Gautier, S., Sandana, V.E, Jomard, F, Abid, M, Molinari, M and Troyon, M, Epitaxial MOVPE growth of highly c-axis oriented InGaN/GaN films on ZnO-buffered Si (111) substrates, *International Society for Optics and Photonics*, (2010), 76031D-76031D
- [34] Tsai, C M, Sheu, J.K., Wang, P.T., Lai, W C, Shei, S C, Chang, S.J, Kuo, C.H., Kuo, C.W. and Su, Y.K, 2006, High efficiency and improved ESD characteristics of GaN-based LEDs with naturally textured surface grown by MOCVD, *IEEE photonics technol. lett*, vol. 18(11), pp.1213-1215
- [35] Chen, Z., Su, L.W., Shi, J.Y., Wang, X.L., Tang, C.L. and Gao, P., AFM application in III-nitride materials and devices. In *Atomic Force Microscopy-Imaging, Measuring and Manipulating Surfaces at the Atomic Scale*. InTech, 2012
- [36] Ng, H. M., Moustakas, T. D., and Ludwig Jr, K. F, Structural and optical characterization of InGaN/GaN multiple quantum wells grown by molecular beam epitaxy, *J.Vac. Sci. & Technol B*, 18(3), (2000) 1457-1460
- [37] Liu, W., Yang, J., Zhao, D., Jiang, D., Zhu, J., Chen, P., Liu, Z., Liang, F., Liu, S., Xing, Y. and Zhang, L., 2018. Energy band tilt in ultra-thin InGaN film affected by the surface adsorption and desorption, *Appl. Surf. Sci*, 456, (2018), 487-492
- [38] Chen, Y., Wu, H., Yue, G., Chen, Z., Zheng, Z., Wu, Z., Gang Wang, and Jiang, H, Enhanced Mg Doping Efficiency in p-Type GaN by Indium-Surfactant-Assisted Delta Doping Method, *Appl. Phys. Express*, 6(4), (2013) 041001

- [39] Kaufmann, U., Kunzer, M., Maier, M., Obloh, H., Ramakrishnan, A., Santic, B., and Schlotter, P, Nature of the 2.8 eV photoluminescence band in Mg doped GaN, Appl. Phys. Lett, 72(11), (1998) 1326-1328
- [40] Correia, M. R., Pereira, S. M. D. S., Pereira, E., Ferreira, R. S., Frandon, J., Alves, E., Watsonf, I.M, Liuf, C. Morel, A and Gil, B, Optical studies on the red luminescence of InGaN epilayers, Superlattices Microstruct, 36(4), (2004) 625-632
- [41] Obloh, H., Bachem, K. H., Kaufmann, U., Kunzer, M., Maier, M., Ramakrishnan, A., and Schlotter, P, Self-compensation in Mg doped p-type GaN grown by MOCVD, J. Cryst. Growth, 195, (1998) 270-273
- [42] Ju, J., Zhu, J., Kim, H., Lee, C., and Lee, I, Effects of p-GaN growth temperature on a green InGaN/GaN multiple quantum well, J. Korean Phys. Soc, 50(3), (2007) 810

Highlights

- Strained InGaN/GaN MQW structures were grown on the sapphire substrates by MOCVD
- Self-organized In(Ga)N like nanostructures and spiral growth were observed in p-GaN
- High intensity green emission was observed for five periods of InGaN/GaN MQWs
- Morphology of V-pit along with emission from nanostructures is discussed
- Hall measurements of p-GaN on InGaN/GaN MQWs exhibits the semiconducting behavior